Economic Geology, v. 103, pp. 1203–1218

Archean Synvolcanic Intrusions and Volcanogenic Massive Sulfide at the Genex Mine, Kamiskotia Area, Timmins, Ontario

S. M. Finamore (Hocker),† H. L. Gibson, and P. C. Thurston

Mineral Exploration Research Centre, Department of Earth Sciences, Laurentian University, 933 Ramsey Lake Road, Sudbury, Ontario, Canada P3E 6B5

Abstract

U-Pb geochronology and detailed field mapping has resulted in a new subdivision of the Kamiskotia Volcanic Complex into Lower and Upper Kamiskotia strata with a 3.5-m.y. volcanic hiatus between the two. The hiatus is interpreted as an unconformity, in common with newly recognized unconformities throughout the greenstone belt. The Genex, and other volcanogenic massive sulfide (VMS) deposits in the area, occur within the Upper Kamiskotia strata. Volcanic facies mapping and reconstruction indicate that the Genex VMS deposit formed within a volcanic graben where synvolcanic mafic and intermediate sills and dikes, with peperitic and locally pillowed contacts, define a proximal volcanic vent area. Sulfide mineralization at Genex occurs in three zones, the first hosted in pillow breccia and hyaloclastite, the second occurring at the contact between felsic tuff and an intermediate intrusion, and the third hosted within the intermediate intrusion. The mineralization represents subsea-floor replacement sulfides localized within zones of higher primary permeability.

Although the synvolcanic mafic intrusions are not directly related to the Genex VMS mineralization they are indicative of a high heat-flow thermal regime. The synvolcanic faults that controlled the emplacement of synvolcanic dikes also provided conduits for the hydrothermal fluids responsible for the mineralization and alteration at Genex. This high-level mafic dike and sill complex was previously correlated with the upper zone of the Kamiskotia Gabbroic Complex but is now interpreted to be younger and correlative with the Upper Kamiskotia Volcanic Complex.

New geochronological data also indicate that the Kamiskotia Gabbroic Complex is older than the VMS-hosting Upper Kamiskotia strata and was emplaced into the Lower Kamiskotia Volcanic Complex. This negates the possibility of a genetic relationship between the Genex and other Kamiskotia VMS deposits within the Kamiskotia Gabbroic Complex. The small size of the synvolcanic intrusions indicates that they were also not the heat source for the Genex hydrothermal alteration system. However, their spatial coincidence suggests that this part of the Kamiskotia Volcanic Complex was the focus of long-lived intrusive activity and high heat flow that defined a thermal corridor encompassing the VMS deposits in the Kamiskotia Volcanic Complex.

Introduction

Between 1964 and 1966 the Genex volcanogenic massive sulfide (VMS) deposit produced 47,000 metric tons (t) of ore at 2.92 percent Cu (or 242 t of copper concentrate at 21 to 27% Cu); zinc was not recovered (*The Northern Miner*, September 1, 1966, p. 13; Middleton, 1975; Legault, 1985; Binney and Barrie, 1991). The deposit is located about 16 km west of Timmins, Ontario (see Hathway et al., 2008), within an Archean, bimodal metavolcanic succession cut by numerous synvolcanic sills and subvolcanic intrusions (Figs. 1, 2). This paper describes the subvolcanic intrusions associated with the Genex deposit and provides evidence for their synvolcanic timing, establishes the spatial and temporal relationship of the intrusions to the Genex VMS mineralization, discusses the potential role of the subvolcanic Kamiskotia Gabbroic Complex and the Genex subvolcanic intrusion as heat sources for the Genex hydrothermal system and their temporal relationships to the Genex stratigraphy, and briefly discusses the implications for correlations with the Blake River assemblage. The findings are based on detailed surface mapping (1:1000, 1:100, and 1:50 scale), logging of 10,225 m of diamond drill core (28 holes), petrographic and geochemical analysis of the volcanic rock types and alteration assemblages, an assessment of the deformation, and new U-Pb geochronology for the Genex volcanic succession and the Kamiskotia Gabbroic Complex.

† Corresponding author: e-mail, steph_finamore@yahoo.com

Regional Geology

Abitibi greenstone belt

The Archean Abitibi greenstone belt of the Archean Superior province is the largest coherent greenstone belt in the world, extending from northeastern Ontario to northwestern Quebec (Dostal and Mueller, 1997; Wyman et al., 2002). The belt is unique in that it contains many predominantly volcanic units all emplaced over a relatively short time span (2750–2696 Ma) with minor associated sedimentary rocks and numerous granitic intrusions (Ayer et al., 2002; Chown et al., 2002).

The western part of the Abitibi greenstone belt experienced semicontinuous subalkalic volcanism from 2750 to 2697 Ma, with komatiitic, tholeiitic, and calc-alkaline magma represented (Ayer et al., 2002). The onset of deformation is constrained to 2696 to 2690 Ma (Ayer et al., 2005). Numerous granitic plutons and batholiths are present throughout the Abitibi and are coeval with volcanism and subsequent tectonic events (Ayer et al., 2002; Chown et al., 2002). The belt is interpreted to have formed over a low-angle, north-dipping Archean subduction zone as a broad oceanic arc, which was then interpreted to have been enhanced and modified by mantle plume processes (Dostal and Mueller, 1997; Ayer et al., 2002; Wyman et al., 2002).

Ayer et al. (2002) subdivided the southern Abitibi greenstone belt into nine supracrustal assemblages on the basis of

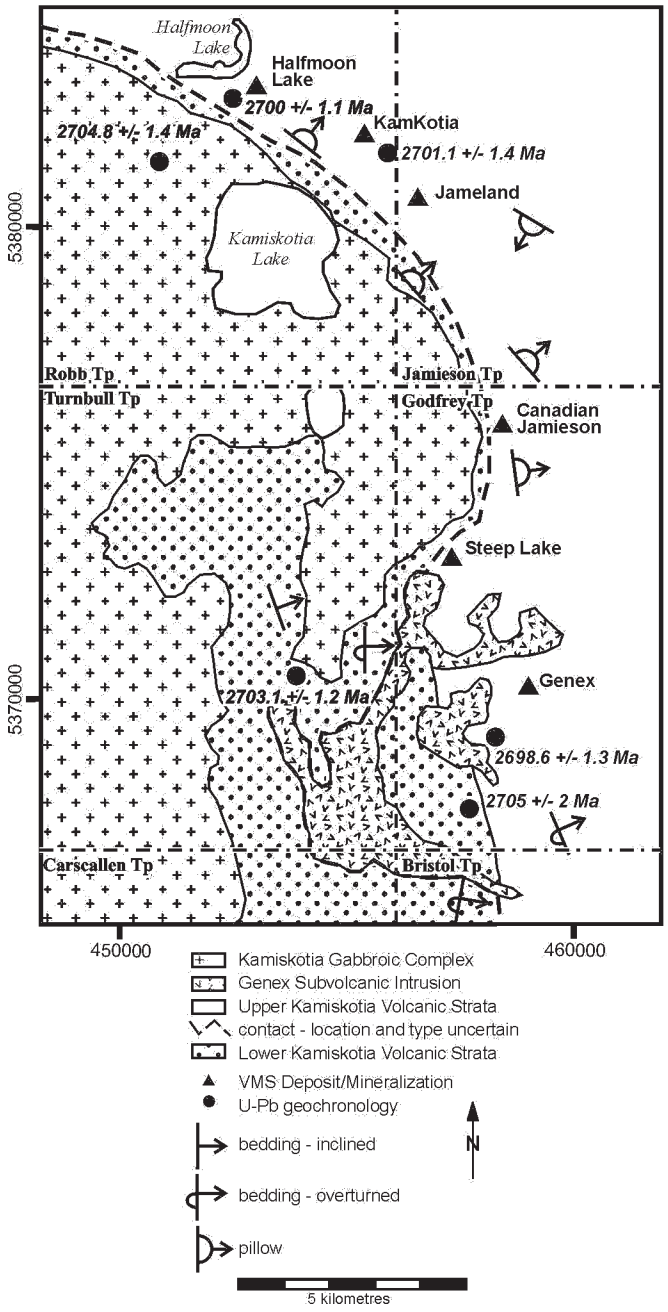

FIG. 1. Geology of the Kamiskotia area, showing the relationship between Lower Kamiskotia strata, Upper Kamiskotia strata, the Kamiskotia Gabbroic Complex, and various synvolcanic intrusions. The sampling points for geochronological samples are indicated. See Hathway et al. (2005) for regional context.

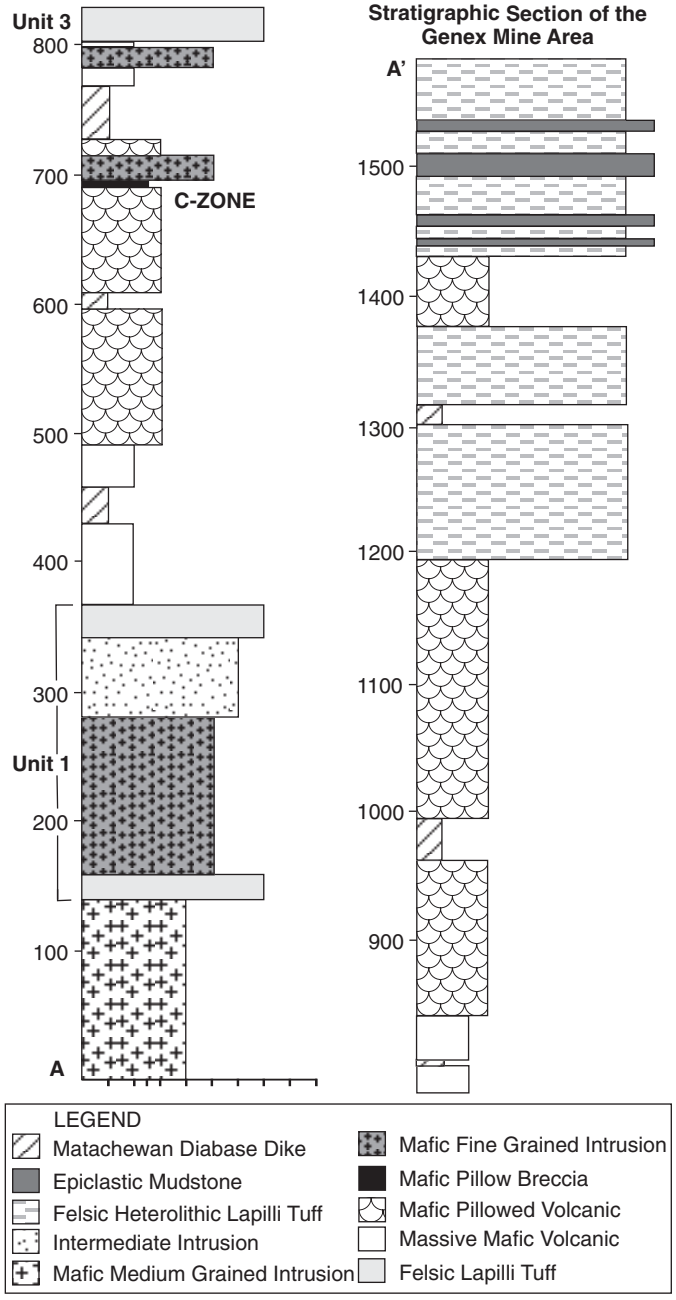

FIG. 2. Stratigraphic section through the Genex stratigraphy (refer to Fig. 3 for location of section). Note that the A and H zones of the Genex deposit do not fall along the section line.

lithology and geochronology. The Genex deposit and the Kamiskotia Volcanic Complex had previously been included in the 2710 to 2703 Tisdale assemblage (Ayer at al., 2002).

Kamiskotia Volcanic Complex

The Kamiskotia Volcanic Complex (Hathway et al., 2008; Fig 1) lies within the westernmost extension of the Archean Abitibi greenstone belt, near Timmins, Ontario (Barrie, 1992). The Kamiskotia Volcanic Complex is a largely homoclinal, eastward younging, bimodal succession of greenschist facies metavolcanic rocks, with minor associated metasedimentary rocks and several large, multiphase (gabbroic to granitic) intrusions (Legault, 1985; Barrie, 1992). The Kamiskotia Volcanic Complex was formerly interpreted to be of Tisdale (2710–2703 Ma) age (Ayer et al., 2002). However, recent field work and U-Pb zircon geochronology (Hathway et al., 2005, 2008; Hocker, 2005; Hocker et al., 2005) have shown that the Genex rocks (part of the Kamiskotia Volcanic Complex) (2698.6 ± 1.3 Ma), as well as a portion of the Kamiskotia Volcanic Complex, are similar in age to the Blake

River Group, located farther to the east (2699 Ma) Regional mapping has indicated that part of the Kamiskotia Volcanic Complex may represent a caldera-type environment (Hathway et al., 2008).

Four past-producing volcanogenic massive sulfide deposits (VMS) occur in the Kamiskotia Volcanic Complex (Legault, 1985; Binney and Barrie, 1991; Fig. 1): (1) the Kam-Kotia deposit (6.0 Mt at 1.09% Cu, 1.03% Zn, 3.5 g Ag/t), (2) the Jameland deposit (461,800 t at 0.99% Cu, 0.88% Zn, 3.5 g Ag/t), (3) the Canadian Jameson deposit (826,400 t at 3.5% Zn, 2.3% Cu), and (4) the Genex deposit (47,000 t of ore at 2.92% Cu).

Genex Stratigraphy

The Genex deposit is located in the southeastern portion of the Kamiskotia Volcanic Complex (Fig. 1) and occurs within an approximately 2-km-thick, north-trending, east-facing volcanic succession that is steeply dipping to slightly overturned, herein referred to as the Genex succession (Figs. 2, 3). Stratigraphic subdivision within the Genex succession is based on outcrop mapping and diamond drill core logging. The base of the volcanic succession is arbitrarily defined by the upper intrusive contact of a medium-grained, mafic intrusion that has traditionally been interpreted as a phase of the Kamiskotia Gabbroic Complex by Middleton (1975), Barrie and Davis (1990), Barrie et al. (1991, 1993), and Barrie (1992). In this study, it is interpreted as a separate, younger intrusion referred to as the Genex subvolcanic intrusion. The top of the volcanic succession is defined by a change from volcanic flows to heterolithic volcaniclastic strata (Fig. 3). Volcanic units within the Genex succession are included within what is termed herein as Upper Kamiskotia strata (a subdivision within the Kamiskotia Volcanic Complex).

The Genex succession can be broadly subdivided into three major units: a lower felsic volcanic unit, a middle mafic volcanic unit, and an upper heterolithic volcaniclastic and epiclastic unit. Numerous intrusions transect all three units. Felsic rocks are dominantly dacite and/or rhyolite in composition; both hanging-wall and footwall mafic rocks are dominantly basaltic andesite in composition (Fig. 4).

Lower felsic volcanic rocks

Felsic volcanic rocks dominate in the Genex area. Lithofacies consist of rhyolitic and rhyodacitic tuff and lapilli tuff, to coherent flows and associated flow breccias that define a generally fining-upward succession. Felsic volcaniclastic rocks are described using Fisher's (1966) nongenetic, granulometric classification, and selected major and trace element analyses are listed in Table 1. All felsic lithofacies have sharp contacts and are grouped into three stratigraphic units (Fig. 3): Unit 1 is a laterally extensive footwall felsic unit, unit 2 is a fault-bounded felsic unit in the immediate footwall, and unit 3 is the felsic unit in the hanging wall of the Genex deposit. Units 1 and 3 are shown in Figure 2; unit 2 does not occur along the section line.

Tuff breccia is common at the base of unit 1, whereas lapilli tuff and tuff occur in both the footwall and hanging wall of the Genex deposit (units 1, 2, and 3). The tuff breccia facies contains lapilli- to block-size fragments that are locally flow banded and commonly compositionally identical to their ma-

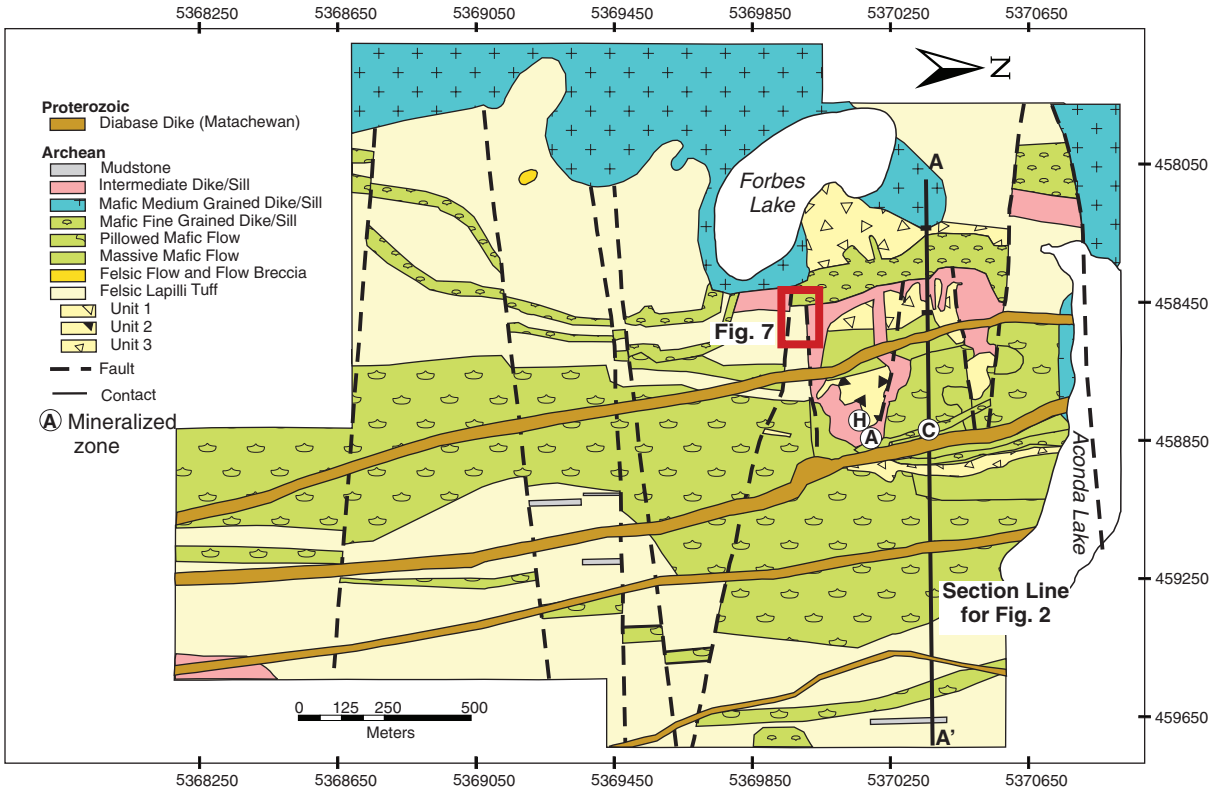

FIG. 3. Geologic map of the Genex area (1:12000 scale). Epiclastic mudstone contacts projected from drill core.

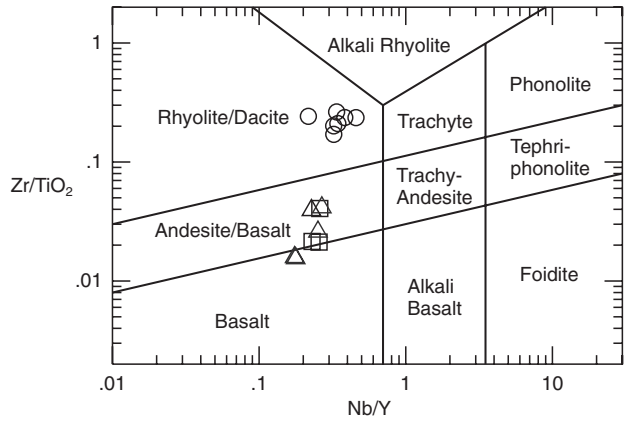

FIG. 4. Discrimination diagram of lithologic units present in the Genex area (see Table 1) for analyses. Circles = felsic rocks, squares = hanging-wall mafic rocks, triangles = footwall mafic rocks.

trix (Fig. 5A). The lapilli-tuff facies is commonly normally graded and crossbedded, although bedding is commonly contorted and discontinuous. Lapilli include altered pumice, silicified felsic lithic fragments, chloritized mafic lithic fragments, altered volcanic glass, and felsic lithic fragments of the same composition as the matrix. Clast size and morphology of each fragment type are highly variable (~1–30 cm, average clast is lapilli sized). Quartz phenocrysts are present in all felsic clasts and are highly microfractured and locally broken. Spherulites occur in the matrices of some lapilli-tuff units indicating an original glassy component of the ash-sized matrix. The ash-sized matrix of the lapilli-tuff and tuff facies is commonly pervasively silicified, sericitized, and locally carbonatized. Quartz crystals constitute up to 15 vol percent of the matrix.

The overall lack of internal bedding and the significant thickness of the felsic breccia (over 800 m thick), especially at

TABLE 1. Geochemistry of Selected Metavolcanic Rocks and Synvolcanic Intrusions from the Genex Area

	FW mafic volcanic					HW mafic volcanic			Felsic volcanic						
Wt %	03-SMH-0001H	03-SMH-0057-3	03-SMH-0082-2	03-SMH-0167	04-SMH-0015-1	03-SMH-0113	03-SMH-0142-1	04-SMH-0005-1	03-SMH-0109-2	03-SMH-0110-1	03-SMH-0112-1	03-SMH-0112-4	03-SMH-0115-1	03-SMH-0140-1	03-SMH-0157
SiO_2	60.52	53.63	61.03	58.90	57.85	53.30	56.38	60.95	76.08	78.56	75.87	73.71	89.17	81.27	73.11
TiO_2	1.85	1.90	0.99	1.37	1.03	1.60	1.86	1.09	0.26	0.22	0.18	0.24	0.13	0.19	0.34
Al_2O_3	12.50	13.29	13.02	11.82	13.19	12.33	14.00	13.38	11.02	10.03	8.18	10.93	6.11	9.07	11.17
Fe_2O_3	7.09	14.20	9.38	9.33	9.99	11.51	10.70	10.30	3.75	3.12	3.57	3.59	1.05	3.36	4.08
FeO	6.38	12.78	8.44	8.40	8.99	10.36	9.63	9.27	3.37	2.81	3.21	3.23	0.94	3.02	3.67
MnO	0.12	0.22	0.18	0.34	0.14	0.41	0.30	0.16	0.09	0.02	0.11	0.06	0.04	0.04	0.10
MgO	3.22	4.52	6.88	2.25	2.68	2.04	1.64	2.62	0.86	1.88	2.53	2.56	0.30	1.84	2.62
CaO	5.07	7.34	4.48	6.36	5.30	7.75	4.17	2.51	0.96	0.42	2.50	1.16	0.41	0.82	1.60
Na_2O	3.92	2.42	1.02	2.87	4.01	2.57	2.62	5.19	3.72	3.53	1.78	4.67	0.08	0.30	0.03
K_2O	0.91	0.02	1.11	0.97	0.74	0.88	1.99	0.48	1.32	0.88	1.41	0.25	1.86	2.15	3.19
P_2O_5	0.20	0.17	0.22	0.47	0.24	0.43	0.47	0.23	0.04	0.03	0.03	0.03	0.03	0.03	0.05
LOI	4.87	4.40	2.99	6.08	3.73	8.11	6.41	2.25	2.11	1.88	4.68	2.85	1.33	2.09	3.93
Total	100.27	102.11	101.30	100.76	98.90	100.93	100.54	99.16	100.21	100.57	100.84	100.05	100.51	101.16	100.22
Ppm															
Cr	36.0	14.0	29.0		23.0		-8.0	9.0	7.0	13.0	12.0	14.0	14.0	12.0	18.0
Ni	12.0	15.0	18.0	7.0	12.0	4.0	-4.0	10.0	2.0			-4.0		4.0	
Co	29.0	33.0	25.0	33.0	N.M.	26.0	N.M.	N.M.				N.M.			
Sc	63.0	49.0	22.0	48.0	N.M.	59.0		N.M.	22.0	23.0	40.0	N.M.	18.0	35.0	34.0
V	405	398	60.0		99.0	64.0	140	110	10.0			11.0			
Cu	27.0	23.0	20.0	21.0	N.M.	27.0	N.M.	N.M.	4.0	6.0	2.0	N.M.		2.0	19.0
Pb			7.0	7.0	N.M.		N.M.	N.M.		14.0	6.0	N.M.		5.0	7.0
Zn	142	121	131	98.0	N.M.	120	N.M.	N.M.	73.0	77.0	62.0	N.M.	54.0	69.0	130
Rb	23.07	0.45	23.55	41.79	18.80	27.64	54.46	10.86	71.57	42.01	43.85	6.26	45.77	41.89	78.50
Cs	0.271	0.034	0.650	0.788	0.792	0.442	1.177	0.626	1.666	0.967	0.628	0.103	0.589	0.849	0.549
Ba	374		246	841	N.M.	211	N.M.	N.M.	275	159	123	N.M.	376	254	311
Sr	30.6	187.2	64.3	116.1	150.3	99.1	85.8	46.4	33.6	47.5	28.3	27.2	13.3	21.3	7.0
Ga	21.0	22.0	20.0	17.0	N.M.	18.0	N.M.	N.M.	17.0	11.0	11.0	N.M.	9.0	14.0	18.0
Ta	0.65	0.65	0.68	0.63	0.62	0.64	0.66	0.67	1.55	1.49	1.06	1.28	0.87	1.13	1.35
Nb	7.1	7.6	9.4	9.0	9.3	9.0	10.1	10.2	19.7	22.1	15.2	19.3	11.8	13.7	18.6
Hf	4.6	4.9	6.3	5.4	6.1	5.3	5.9	6.7	9.5	9.6	8.2	9.7	5.7	7.5	9.9
Zr	171.2	179.7	245.5	212.3	242.2	206	236.5	265.3	313.4	310.9	284.5	348.3	184.3	239.8	348.2
Y	39.95	43.51	35.1	35.67	40.84	39.2	39.35	39.28	61.06	48.3	45.01	89.09	30.73	39.81	57.56
Th	1.69	1.76	2.98	2.26	2.75	2.27	2.59	2.90	6.88	6.21	4.60	5.86	4.10	5.72	5.79
U	0.461	0.476	0.764	0.631	0.708	0.585	0.636	0.739	1.67	1.585	1.121	1.504	1.005	1.275	1.291
La	14.88	13.3	21.67	17.07	21.28	21.28	20.02	22.6	41.6	48.7	33.05	40.21	58.51	42.96	38.36
Ce	34.31	32.34	50.79	40.03	49.36	49.9	48.6	53.92	93.59	108.91	74.96	88.63	112.01	98.31	88.27
Pr	4.709	4.525	6.694	5.405	6.554	6.727	6.484	7.235	11.656	13.992	9.462	11.102	13.059	12.535	11.043
Nd	21.07	20.76	28.95	24.61	28.29	29.52	28.57	30.74	46.72	56.38	39.01	45.91	45.83	50.93	45.77
Sm	5.58	5.65	6.8	6.04	6.72	7.05	6.79	7.13	10.11	12.49	8.58	10.44	7.36	10.82	10.44
Eu	1.782	1.817	1.75	1.676	1.645	1.829	1.777	1.382	1.375	1.778	1.387	1.735	1.239	1.585	1.785
Gd	6.692	6.809	6.903	6.87	7.26	7.766	7.212	7.35	10.724	12.47	8.456	11.808	6.779	9.607	10.751
Tb	1.125	1.169	1.056	1.112	1.18	1.183	1.147	1.198	1.781	1.911	1.323	2.108	0.963	1.33	1.781
Dy	7.126	7.507	6.367	6.86	7.3	7.177	7.049	7.42	11.159	10.749	8.152	14.405	5.898	7.707	10.858

TABLE 1. *(Con't)*

	FW mafic volcanic					HW mafic volcanic				Felsic volcanic					
Wt %	03-SMH-0001H	03-SMH-0057-3	03-SMH-0082-2	03-SMH-0167	04-SMH-0015-1	03-SMH-0113	03-SMH-0142-1	04-SMH-0005-1	03-SMH-0109-2	03-SMH-0110-1	03-SMH-0112-1	03-SMH-0112-4	03-SMH-0115-1	03-SMH-0140-1	03-SMH-0157
Ho	1.479	1.627	1.334	1.403	1.487	1.477	1.478	1.477	2.347	2.039	1.709	3.156	1.239	1.558	2.265
Er	4.35	4.871	3.984	4.124	4.41	4.292	4.361	4.29	7.036	5.541	5.098	9.54	3.765	4.702	6.846
Tm	0.626	0.725	0.6	0.598	0.656	0.629	0.642	0.634	1.035	0.789	0.77	1.413	0.582	0.706	1.062
Yb	3.97	4.71	4.04	3.81	4.29	4.02	4.24	4.13	6.55	5.09	5.05	9.08	3.87	4.74	7.17
Lu	0.594	0.721	0.619	0.559	0.639	0.62	0.639	0.622	0.971	0.752	0.76	1.337	0.583	0.702	1.101
(La/Sm) CN	4.13	3.65	4.94	4.38	4.91	4.68	4.57	4.91	6.37	6.04	5.97	5.97	12.31	6.15	5.69
Eu/Eu*	0.10	0.10	0.08	0.09	0.08	0.08	0.08	0.06	0.04	0.05	0.05	0.05	0.06	0.05	0.06

	Mafic intrusion								Intermediate intrusion				
Wt %	03-SMH-0007	03-SMH-0030	03-SMH-0112-5	04-SMH-0001-22	04-SMH-0003-7	04-SMH-0004-1	04-SMH-0027-1	04-SMH-0071-1	03-SMH-0024	03-SMH-0028-1	03-SMH-0053	03-SMH-0111-4	04-SMH-0023-2
SiO_2	49.98	50.19	43.85	48.73	50.82	50.97	44.25	46.46	59.20	60.79	48.59	63.11	46.01
TiO_2	1.29	1.34	1.17	1.34	1.33	1.43	1.05	1.13	1.07	0.90	0.82	0.88	1.25
Al_2O_3	13.56	13.74	13.64	14.44	13.65	14.72	14.72	12.40	13.39	11.40	10.64	12.87	14.98
Fe_2O_3	14.42	14.72	12.41	14.00	11.36	12.04	12.14	12.92	10.58	9.18	10.25	6.99	14.69
FeO	12.98	13.25	11.17	12.60	10.22	10.83	10.92	11.63	9.52	8.26	9.22	6.29	13.22
MnO	0.24	0.14	0.21	0.27	0.25	0.27	0.17	0.17	0.09	0.21	0.09	0.07	0.16
MgO	6.57	8.13	4.72	6.86	4.72	6.28	6.30	6.36	7.36	5.23	8.20	2.11	7.18
CaO	8.68	5.56	10.17	6.40	10.07	6.66	7.36	6.89	1.20	4.40	6.29	3.11	7.05
Na_2O	3.20	3.78	2.33	2.85	1.40	3.90	3.74	2.80	2.22	2.59	2.31	4.79	2.85
K_2O	0.20	0.07	0.92	2.62	0.04	0.69	0.26	0.25	0.52	0.31	0.60	0.93	0.32
P_2O_5	0.09	0.12	0.11	0.12	0.13	0.13	0.08	0.13	0.18	0.18	0.17	0.19	0.12
LOI	3.33	4.16	10.85	2.83	5.91	1.74	9.36	10.90	5.40	6.13	13.33	5.25	4.11
Total	101.56	101.95	100.38	100.46	99.68	98.83	99.43	100.41	101.21	101.32	101.29	100.30	98.72
Ppm													
Cr	126	121	110	96.0	95.0	98.0	224	100	26.0	22.0	15.0	-8.0	33.0
Ni	43.0	44.0	74.0	50.0	40.0	40.0	129	44.0	16.0	13.0	14.0	7.0	26.0
Co	53.0	49.0		N.M.	N.M.	N.M.	N.M.	N.M.	23.0	28.0	15.0	N.M.	N.M.
Sc	57.0	67.0	N.M.	N.M.	N.M.	N.M.	N.M.	N.M.	45.0	48.0	38.0	N.M.	N.M.
V	270	315	356	337	303	385	222	328	68.0	53.0	37.0	106	140
Cu	105	106	N.M.	N.M.	N.M.	N.M.	N.M.	N.M.	8.0	51.0	36.0	N.M.	N.M.
Pb			N.M.	N.M.	N.M.	N.M.	N.M.	N.M.	5.0	6.0		N.M.	N.M.
Zn	100	96.0	N.M.	N.M.	N.M.	N.M.	N.M.	N.M.	388	144	107	N.M.	N.M.
Rb	3.38	1.28	30.87	42.82	0.44	6.43	6.28	7.38	15.15	5.73	11.31	19.18	35.36
Cs	0.186	0.233	0.482	0.427	0.215	0.366	0.302	0.264	0.193	0.164	0.113	0.453	0.451
Ba	72.0	72.0	N.M.	N.M.	N.M.	N.M.	N.M.	N.M.	45.0	75.0	93.0	N.M.	N.M.
Sr	101.6	119.4	111.5	98.6	302.2	65.1	229.0	178.3	32.8	62.7	104.2	108.2	10.9
Ga	17.0	20.0	N.M.	N.M.	N.M.	N.M.	N.M.	N.M.	21.0	15.0	15.0	N.M.	N.M.
Ta	0.35	0.38	0.22	0.29	0.25	0.25		0.24	0.81	0.70	0.69	0.71	0.58
Nb	3.5	3.9	3.5	4.3	4.0	4.1	1.7	3.7	9.9	7.8	7.8	9.6	8.3
Hf	2.2	2.6	2.3	2.6	2.7	3.5	1.5	2.5	6.7	5.2	5.4	5.9	5.3
Zr	83.8	93.4	86.0	97.4	100.5	134.5	51.7	91.7	261.7	202.8	213.3	228.6	212.6
Y	24.08	26.83	23.76	27.72	28.52	27.68	18.49	21.76	35.74	32.49	35.18	27.86	17.49
Th	0.55	0.65	0.54	0.64	0.63	0.61	0.45	0.60	2.90	2.38	2.33	3.44	2.19
U	0.153	0.171	0.139	0.168	0.171	0.17	0.1	0.151	0.753	0.632	0.615	0.866	0.563
La	5.69	6.85	5.79	7.42	6.86	6.41	4.79	5.68	12.24	12.68	15.3	23.94	12.29
Ce	14.32	16.63	14.21	18.56	16.89	15.45	12.16	13.97	28.66	31.28	37.73	53.87	28.69
Pr	2.064	2.396	2.044	2.7	2.551	2.238	1.783	2.061	3.785	4.225	5.135	6.816	3.714
Nd	10.03	11.57	10.03	13.38	12.13	10.62	8.94	10.13	16.34	18.82	22.49	28.24	15.88
Sm	2.92	3.29	2.87	3.69	3.48	3.14	2.53	2.8	4.27	4.84	5.5	6.1	3.53
Eu	1.002	1.063	0.719	1.112	1.161	1.003	0.906	0.885	0.729	1.256	1.448	1.366	0.817
Gd	3.744	4.318	3.722	4.481	4.4	4.109	2.988	3.483	5.413	5.684	6.18	6.028	3.341
Tb	0.651	0.751	0.626	0.765	0.759	0.728	0.511	0.596	0.981	0.945	1.019	0.918	0.519
Dy	4.21	4.756	4.248	4.934	5.009	4.876	3.242	3.817	6.648	5.886	6.284	5.586	3.193
Ho	0.909	1.035	0.917	1.038	1.084	1.059	0.677	0.833	1.467	1.271	1.303	1.101	0.664
Er	2.7	3.077	2.759	3.13	3.263	3.119	2.02	2.553	4.488	3.778	3.846	3.116	1.986
Tm	0.407	0.462	0.406	0.461	0.481	0.472	0.296	0.381	0.68	0.561	0.566	0.467	0.291
Yb	2.69	2.97	2.68	3.04	3.13	3.07	1.92	2.52	4.62	3.68	3.82	3.12	1.91
Lu	0.406	0.446	0.403	0.465	0.476	0.468	0.284	0.383	0.71	0.563	0.593	0.465	0.276
(La/Sm) CN	3.02	3.23	3.13	3.11	3.05	3.16	2.93	3.14	4.44	4.06	4.31	6.08	5.39
Eu/Eu*	0.10	0.09	0.07	0.09	0.10	0.09	0.11	0.09	0.05	0.08	0.08	0.07	0.08

Notes: UTM locations for samples can be found in Hocker (2005); N.M. = not measured; CN = chondrite normalized (Sun and McDonough, 1989); Eu/Eu* calculated by interpolation between chondrite normalized Sm and Gd (values from Sun and McDonough, 1989; method from Rollinson, 1993)

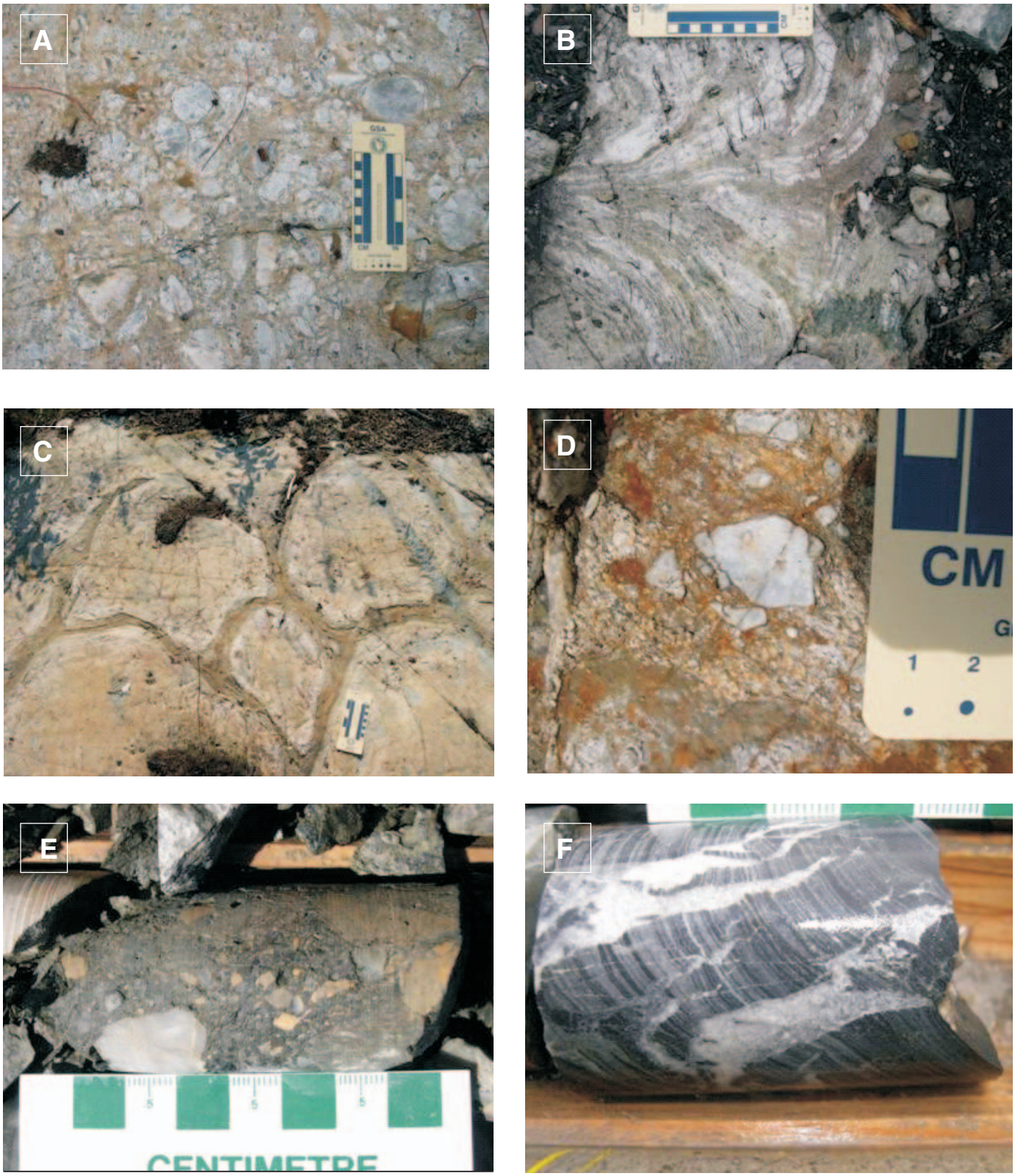

FIG. 5. Outcrop photographs of (A) felsic block and lapilli tuff, (B) flow-banded felsic flow breccia, (C) pillowed mafic flow, (D) pillow breccia with silicified fragments and sulfides in matrix, (E) heterolithic lapilli-tuff breccia, and (F) finely laminated mudstone.

the base of unit 1, suggest that the breccias may be the result of a large collapse event (i.e., caldera collapse: Troll et al., 2000).

The coherent felsic flow and flow breccia facies occur in units 1, 2, and 3 but are much less common than felsic tuff and lapilli-tuff facies. Quartz and feldspar phenocryst content varies between the different flow and flow breccia facies. Flows are commonly flow banded, spherulitic, and locally contain felsic pumice lapilli and lithic fragments in a crystalline, siliceous matrix (Fig. 5B). Flow breccias typically contain angular, flow-banded lapilli and blocks, which locally have a jig-saw fit and a coherent flow-banded matrix. Coarse, block-rich monolithic breccias are flow banded and spherulitic, have similar phenocryst contents, and locally have a jig-saw fit. These breccias are interpreted as in situ or minimally transported autoclastic breccias. The occurrence of such breccia is interpreted to indicate proximity to coherent flows or domes and therefore a vent proximal environment (Gibson et al., 1999).

Middle mafic volcanic rocks

Mafic volcanic rocks occur throughout the Genex area. They are basaltic andesite in composition and consist of pillowed and massive flow facies and minor mafic tuff. Pillowed flows in the footwall of the VMS deposit contain small (~25 cm) well-defined pillows to large (~250 cm) irregularly shaped pillows (Fig. 5C). Hyaloclastite at the pillow margins ranges from ~2 to ~20 cm in thickness and contains well-defined perlitic, cuspate-altered glass shards, and altered glass. Budding and concentric cooling cracks are common. Amygdules are filled by quartz, chlorite, and carbonate. The mineralogy of most samples is now represented by chlorite, epidote, sericite, quartz, and ankerite. Up to 10 vol percent spherulites (millimeter-scale) are locally present.

Pillowed flows in the hanging wall of the deposit show a lesser degree of size variability than their footwall counterparts, ranging in size from ~25 to ~200 cm, and are generally irregularly shaped. Hyaloclastite at the pillow margins ranges from ~1.5 to ~7 cm in thickness and is generally marked by an abundance (up to 90%) of spherulites, giving the selvages a bleached appearance. Budding and concentric cooling cracks are not common. Amygdules are mainly carbonate filled with minor quartz.

Massive mafic units are subdivided into those which are conformable and those which are disconformable. All massive mafic units are fine grained with quartz- and carbonate-filled amygdules. Conformable massive mafic units occur stratigraphically below pillowed flows, often with gradational contacts, indicating that the conformable massive mafic units are the basal flow parts of individual flows (Dimroth et al., 1978). Discordant massive mafic units occur in close proximity to the east-trending faults in the Genex area. These are interpreted as feeder dikes for the mafic flows in the area that utilized the faults as conduits (e.g., Binney and Barrie, 1991; Stix et al., 2003).

Localized pillow breccia units commonly occur at the top of the pillowed facies (Fig. 5D). Flow breccia facies is similar in composition to the flows but also contain highly silicified, amygdaloidal mafic fragments in a fine-grained, quartz-filled amygdaloidal basalt matrix. At the Genex deposit, the C-zone mineralization is hosted within the matrix of one such pillow breccia.

Upper epiclastic and/or volcaniclastic rocks

Volcaniclastic and epiclastic rocks east of the Genex mine area have only been observed in drill core, and their upper contact is not defined due to a lack of outcrop and drill core. However, the succession is at least 600 m thick and is composed of meter-scale, normally graded felsic heterolithic tuff breccia and lapilli tuff, to locally bedded-tuff, to black, finely laminated, locally pyritic, mudstone, or graphitic argillite. The pronounced heterolithologic nature of clasts within the tuff breccia and lapilli-tuff facies suggests that they have a complex, multiple source provenance, and that they are not primary pyroclastic or autoclastic deposits (Fig. 5E). Tuff units commonly contain a minor mudstone component and are locally thinly bedded. Like the coarser units, the heterolithologic nature of clasts within the tuff units suggest multiple sources, which is consistent with the interpretation that they have been redeposited (Gibson et al., 1999). Laminated mudstones or graphitic argillites are black with cross-bedding and soft-sediment deformation structures (Fig. 5F). The graphitic component of the mudstones is likely of hemipelagic origin. The fine grain size and carbonaceous nature of the mudstones suggest they may be epiclastic in origin. The presence of cross-bedding and soft-sediment deformation indicates that the mudstones have been reworked, presumably by bottom currents, and that they have subsequently undergone slumping.

Widespread soft-sediment deformation, graded beds, bedding, and crossbedding, all suggest that the volcaniclastic rocks were deposited as a series of subaqueous mass flows (or low-concentration turbidity currents: cf. Cas and Wright, 1988; White, 2000) during a period of volcanic quiescence. Mudstone beds mark a hiatus in mass-flow sedimentation that allowed relatively calm suspension-deposition of pelagic sediments (Mueller and Mortensen, 2002). The few felsic flows and mafic flows that disrupt the volcaniclastic sequence indicate that limited volcanism was ongoing.

Mafic sills

Fine-grained mafic sills are subdivided on the basis of their stratigraphic position into lower and upper sills. The upper sills occur as two north-trending sills in unit 2, in the immediate hanging wall of the Genex deposit. The lower fine-grained sills occur as two north-trending sills in unit 1. The lower sills locally have numerous small apophyses stemming from the main body. Along strike, to the north, the two lower sills merge into a single sill (Fig. 3).

All the mafic intrusions, including the Genex subvolcanic intrusion (by Forbes Lake, Fig. 3), are gabbro to quartz gabbro in composition, and are characterized by a secondary metamorphic mineral assemblage of epidote, chlorite, quartz, ankerite, sericite, and in one sample, muscovite. In a few samples, remnant primary minerals such as clinopyroxene and plagioclase phenocrysts are present. Up to 5 vol percent spherulites occur locally in the sills (observed in thin section), indicating that the sill was rapidly cooled and originally glass rich (Cas and Wright, 1988). Up to 50 vol percent quartz- and carbonate-filled amygdules occur along the margins of the sills. The lower sills locally have abundant fracture-controlled, stringer sulfide mineralization, whereas the upper sills are not mineralized.

The basal contact of the lower sill is locally pillowed and brecciated, with the breccia containing aphanitic chilled and chloritized, irregularly shaped fragments of the sill (Fig. 6A). The upper contact is also irregular, with numerous dikes stemming from the main intrusive body. These dikes are amoeboid in form and are locally enveloped within peperite

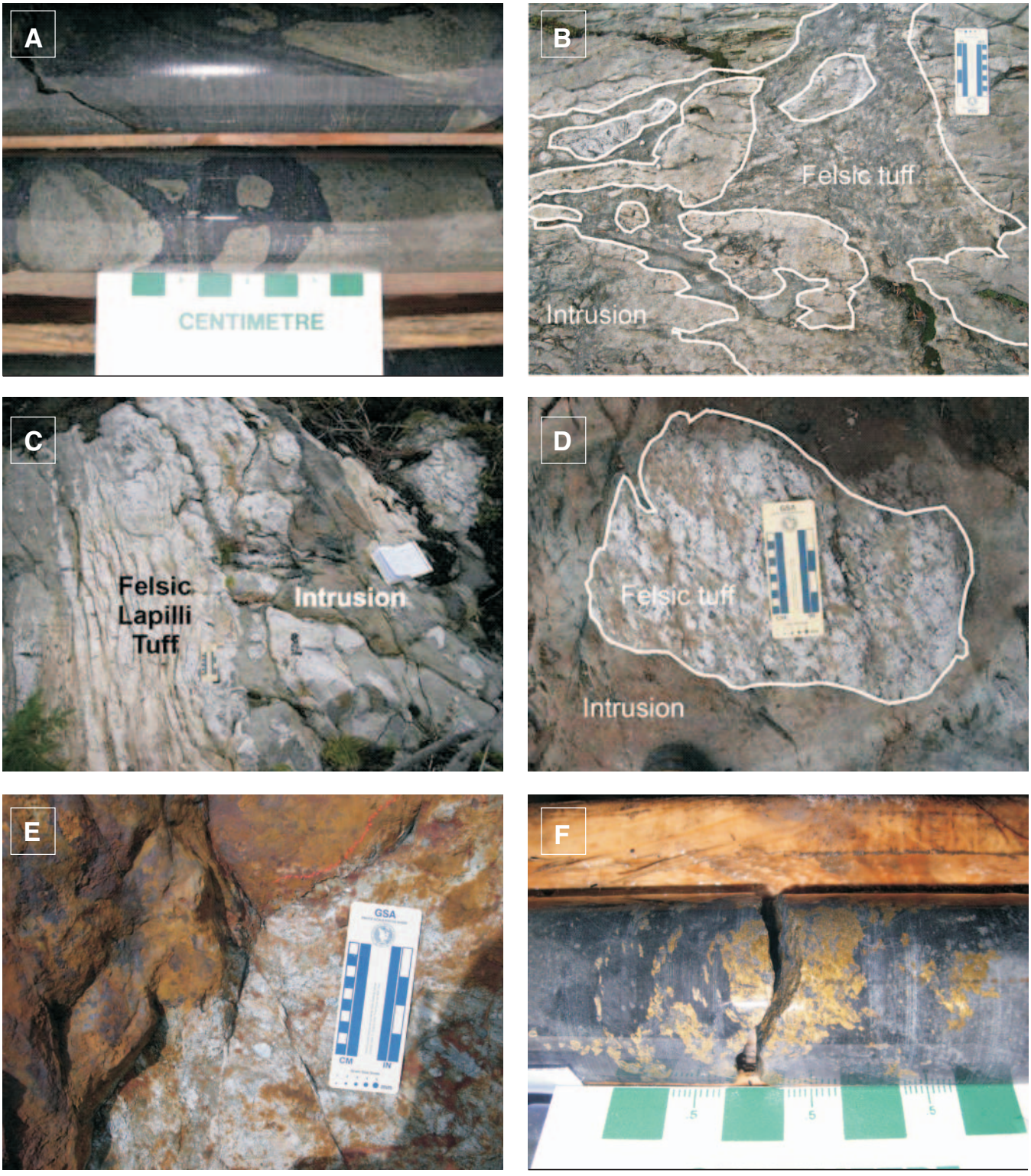

FIG. 6. Photographs of (A) brecciated lower contact of the lower fine-grained mafic intrusion, (B) amoeboid felsic tuff fragments incorporated into mafic intrusion, (C) mixed zone in upper contact of north-trending intermediate intrusion, (D) coherent block of lapilli tuff in upper contact of north-trending intermediate intrusion, (E) mineralized pillow breccia in the C zone, (F) A-zone sulfide mineralization in intermediate synvolcanic intrusion.

where they have intruded felsic volcaniclastic rocks. The sills contain irregular- and amoeboid, lapilli- to block-sized felsic volcaniclastic xenoliths near their upper contacts (Fig. 6B).

The contacts of the upper fine-grained sills are poorly exposed in outcrop. Peperite occurs at the lower contact of the upper sill where lapilli- to block-sized, irregularly shaped fragments of the sill are incorporated in the felsic lapilli tuff. The upper contact is irregular with numerous amoeboid dikes stemming from the main body. The upper fine-grained sill does not contain felsic volcanic xenoliths.

Intermediate sill

Between the upper and lower mafic sill units is an intermediate sill that trends north and has numerous east-trending dikes stemming from the main body that parallel faults in the Genex mine area. The intermediate sill is fine- to coarse-grained, has a composition that ranges from rhyodacite to dacite, and is characterized by a secondary mineral assemblage of ankerite, chlorite, quartz, epidote, and sericite. Primary minerals include plagioclase, quartz, and orthopyroxene phenocrysts, all within a very fine grained groundmass that commonly contains up to 20 vol percent, 1- to 2-mm spherulites, indicating that the sill was rapidly cooled and originally glass rich (Cas and Wright, 1988). Quartz- and carbonate-filled amygdules are locally concentrated along the margins of the east-trending dikes, and polygonal joints occur within the thicker sections of the sill. The sill consists of multiple intrusive phases distinguished by linear zones of in situ breccia that parallel the intrusion margins. The in situ breccia consists of angular fragments of the sill in a finer grained, quartz-rich matrix. The morphology of the fragments, their contact-parallel orientation, and the quartz-rich matrix indicate that the breccia is a product of flow, and possibly quench fragmentation, during sill emplacement.

The lower area of the intermediate sill contact is characterized by numerous apophyses that intrude the underlying volcanic rocks and the lower mafic sill. The upper contact of the north-trending sill, as well as the contacts of the east-trending dikes, is characterized by a mixed zone up to 25 m wide where fragments of the sill and the overlying rocks are chaotically mixed (Fig. 6C). However, unlike the mafic intrusion, xenoliths of felsic tuff within the sill are not amoeboid in form but occur as intact blocks (Fig. 6D). In the immediate footwall of the Genex deposit, the east-trending dikes that stem from the sill are brecciated in situ where in contact with felsic lapilli tuff. The in situ breccia consists of fragments of the intrusion in an altered glass matrix.

Numerous east-trending faults do not offset the sill, but many of the dikes stemming from the sill follow these faults (also described in the Genex area by Binney and Barrie, 1991). The east-trending dikes commonly contain abundant sulfides higher in the mine stratigraphy (below the Genex deposit), whereas the lower parts of the sill are unmineralized.

The intermediate sill is distinguished from the mafic sill by less epidote alteration, a higher degree of carbonate alteration, and a greater abundance of quartz and spherulites.

Late diabase intrusive rocks (Matachewan)

Based on their northerly trend, presence of epidotized plagioclase glomerocrysts, and magnetic nature, the four diabase dikes in the Genex area are interpreted to be part of the Proterozoic (2454 ± 2 Ma: Heaman, 1988) Matachewan dike swarm that intruded the Kamiskotia and surrounding area (Ernst, 1981; Osmani, 1991). In the Genex area, the dikes are fine- to coarse-grained diabase, with plagioclase, quartz, and clinopyroxene phenocrysts. Much of the plagioclase has been altered to epidote, zoisite, and sericite while most of the pyroxene has been altered to chlorite, actinolite, and epidote.

Synvolcanic Timing of Sill Emplacement

Mafic sills

The presence of peperite, a pillowed base, irregular contacts, amoeboid dikelike apophyses, incorporation of irregular xenoliths of felsic volcaniclastic rocks, and their conformable to semiconformable attitude indicate that the lower, fine-grained mafic sills were emplaced into unconsolidated, wet, volcaniclastic rocks (Gibson et al., 1999). The upper, fine-grained mafic sills are similar to their lower counterparts and are also interpreted to be synvolcanic. The absence of felsic xenoliths in the upper mafic sill suggests that they may be slightly younger than the lower mafic sills (i.e., the host rock was more consolidated when it was intruded).

The synvolcanic timing and multiple emplacement history of the mafic sills is illustrated in Figure 7, where the upper contact of the lower mafic sill with an overlying felsic flow breccia is exposed. Here, numerous amoeboid dikes of the mafic sill show a variable degree of interaction as evidenced by irregular contacts with the host felsic volcaniclastic rocks and peperite development in contact with the felsic flow breccia. For example, in Figure 7, the earliest phases of the sill show a high degree of interaction with the unconsolidated felsic flow breccia, including the formation of blocky peperite that developed as the intrusion rapidly quenched and was brecciated in contact with the felsic breccia. The next intrusive phase surrounded and engulfed the peperite but instead of quenching against the felsic flow breccia it incorporated numerous xenoliths of the breccia. Subsequent phases of the sill have sharp and regular contacts with the felsic flow breccia. The shift from irregular to regular contacts and the decrease in peperite formation with each subsequent intrusion is interpreted to be a function of the timing of sill emplacement, such that successive pulses of the intrusion interacted to a decreasing extent with the host rocks as the host became indurated and more consolidated during successive intrusive episodes (cf. Gibson et al., 2003; Houlé et al., 2008).

Intermediate sill

The presence of a mixed zone, abundant spherulites (devitrified glass indicating rapid cooling) and amygdules, in situ brecciated zones within the sill, and the utilization of faults as conduits all suggest that the intermediate sill is a high-level synvolcanic intrusion that was emplaced in unconsolidated strata relatively close (<500 m) to the sea floor (cf. Gibson et al., 1999; Doyle and Allen, 2003).

Unlike the mafic sills, blocks of felsic tuff within the intermediate sill are intact, suggesting that they were partly consolidated prior to incorporation. Furthermore, the intermediate sill is offset by faults, which suggests that the intermediate

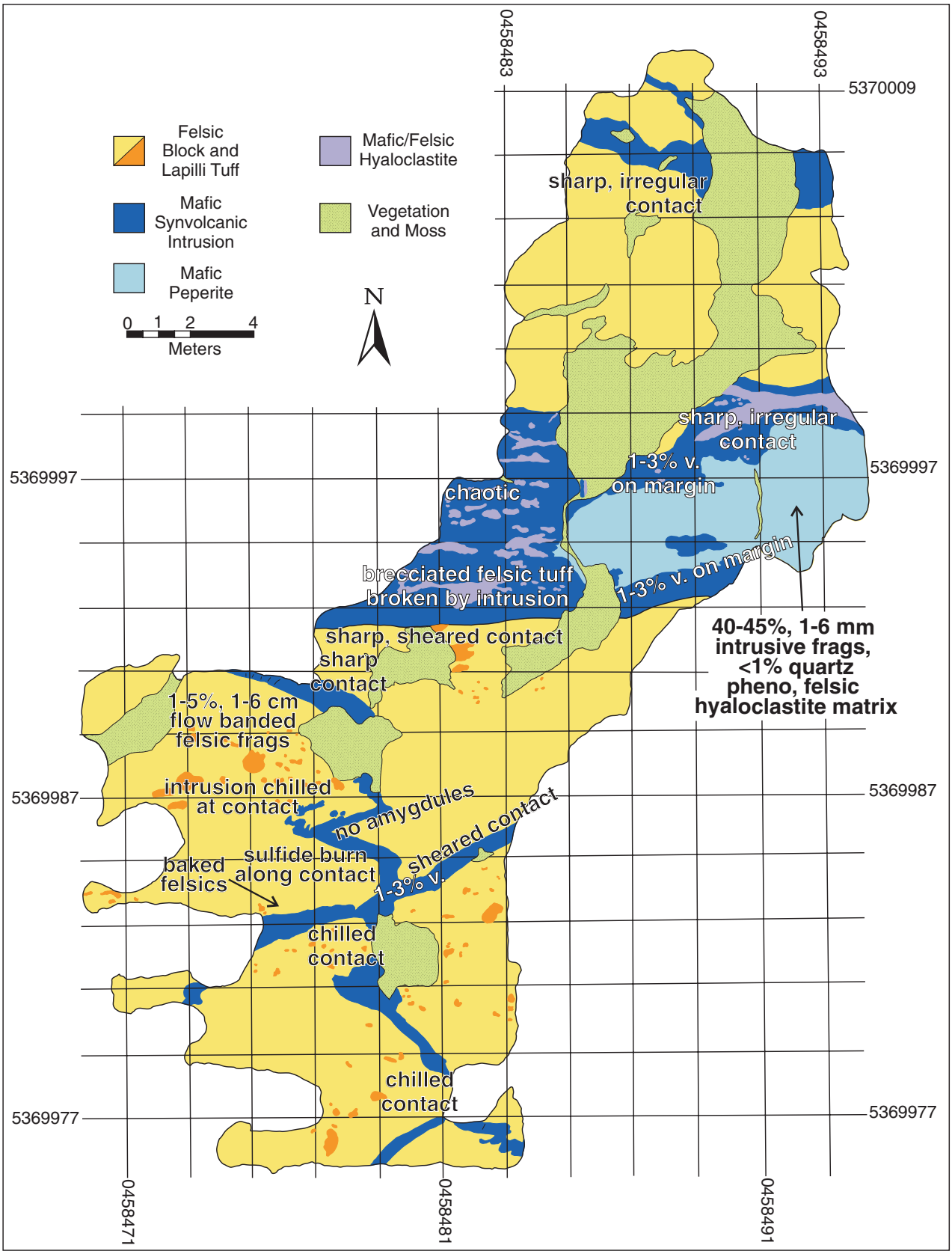

FIG. 7. Scale map (1:50) of contact between synvolcanic mafic intrusion and felsic flow breccia (outcrop 03-SMH-0112); pheno = phenocrysts. Refer to Figure 3 for location.

intrusion is slightly younger than the mafic intrusions, but postdates some of the earlier faulting.

Petrochemistry

One hundred and eighty-five samples were analyzed for major, trace, and rare earth elements (REE), using XRF (fused and pressed pellets) and ICPMS techniques at the Ontario Geoscience Laboratories and Activation Laboratories Limited. Representative geochemical analyses are listed in Table 1. UTM locations, as well as all 185 geochemical analyses and detailed description of analytical procedure can be found in Hocker (2005); precision and accuracy calculations can be found in MacDonald et al. (2005). A selection of 28 analyses is taken to be representative of the least altered compositions of the different rock types discussed. Details of the selection criteria (petrographic and geochemical) can be found in Hocker et al. (2005).

REE

Chondrite-normalized REE plots for Genex mafic volcanic rocks (Fig. 8A) display relatively flat patterns with only a slight enrichment in the LREE, indicating an unevolved and unfractionated magma; the average $(La/Sm)_{chondrite\text{-}normalized}$ ratio for footwall rocks is 4.40, the average $(La/Sm)_{chondrite\text{-}normalized}$ ratio for hanging-wall rocks is 4.72. Hanging-wall and footwall rocks have similar REE abundances; however, the hanging-wall volcanic rocks are slightly more enriched in LREE than the footwall rocks and are likely more fractionated.

In contrast, a chondrite-normalized REE plot of the synvolcanic mafic sills (Fig. 8B) indicates derivation from a more primitive magma relative to the Genex mafic volcanic rocks with an average $(La/Sm)_{chondrite\text{-}normalized}$ ratio of 3.10. Conversely, a chondrite-normalized REE plot of the Genex synvolcanic intermediate sill (Fig. 8C) indicates a more evolved or fractionated magma similar to the mafic volcanic rocks with an average $(La/Sm)_{chondrite\text{-}normalized}$ ratio of 4.86. Eu/Eu* values (Table 1) are consistent with derivation of the synvolcanic mafic sills (avg Eu/Eu* = 0.09) from a more primitive source than the synvolcanic intermediate sills (avg Eu/Eu* = 0.07).

Contamination

Crustal contamination for rocks of basaltic composition can be demonstrated using the Zr-Ti/100-Y*3 ternary plot developed by Pearce and Cann (1973) and modified by Pearce (1996; Fig. 9) where MM is the composition of average N-MORB mantle, and UC represents the composition of average upper crust. For example, a sample that plots near the average N-MORB mantle point is interpreted to have been derived from a mantle melt that did not interact with the crust, whereas a sample that plots near the average upper crust point is derived from a magma that has interacted extensively with the crust or is derived from the crust. For mantle-derived sources, the relative enrichment of the mantle and the degree of melting can also be estimated from the diagram. It is important to note that in interpreting these ternary plots, it is the trends that are important, not where the individual points fall. For example, if a suite of rocks plots on a trend toward upper crustal composition, this is an indication that contamination occurred.

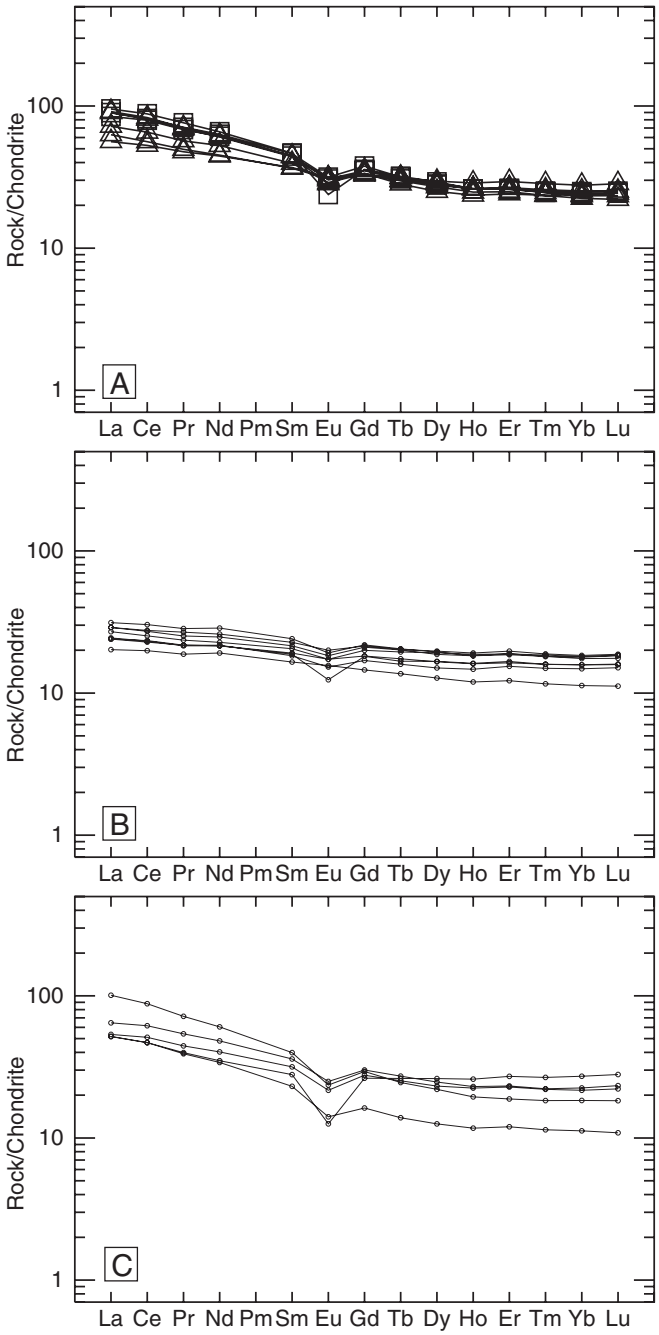

FIG. 8. Chondrite-normalized REE plots of samples from the synvolcanic mafic intrusion (normalizing values after Sun and McDonough, 1989). A. Genex mafic volcanic rocks. Triangles = footwall rocks, squares = hanging-wall rocks. B. Genex synvolcanic mafic intrusion. C. Genex synvolcanic intermediate intrusion.

The Genex mafic volcanic rocks plot in a range from near the average N-MORB mantle to near the average upper crust, suggesting fractionation and variable degrees of crustal contamination (Fig. 9A). Conversely, the synvolcanic mafic sill samples plot almost exclusively near the average N-MORB mantle, suggesting less fractionation and/or crustal contamination than the mafic volcanics (Fig. 9B). This may indicate that the synvolcanic mafic sill was derived from a

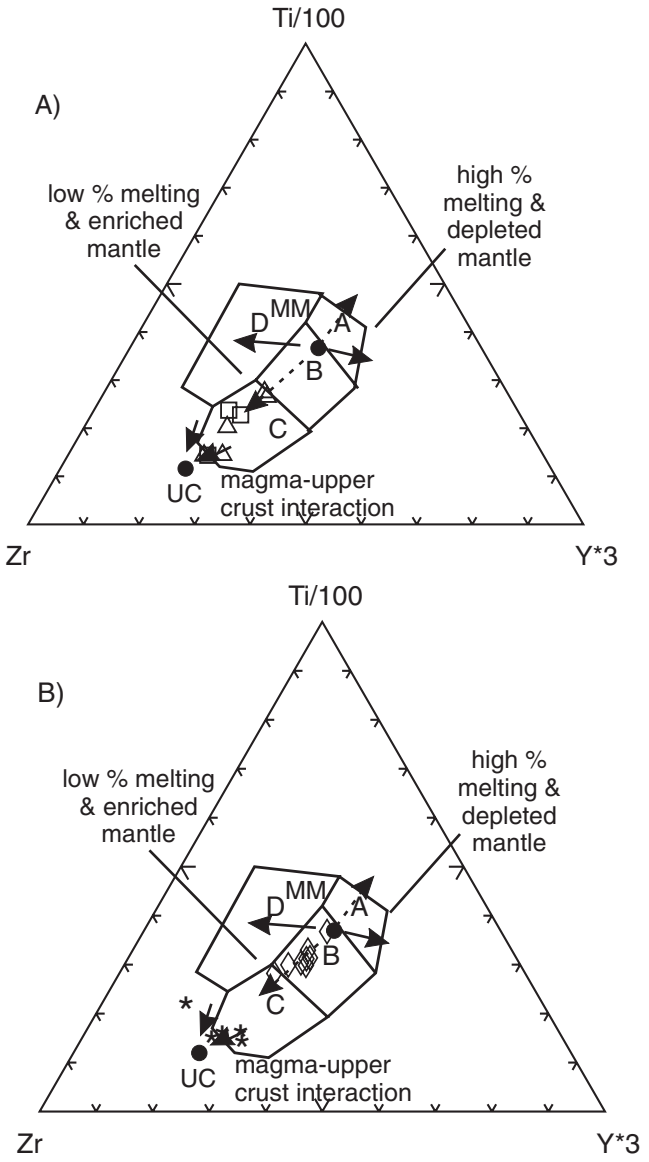

FIG. 9. Zr-Ti/100-Y*3 ternary plots after Pearce (1996) and Pearce and Cann (1973; selected analyses). AB = island-arc, B = ocean-floor, BC = calc-alkali, D = within-plate, MM = average N-MORB mantle, UC = average upper crust. A. Genex mafic volcanic rocks are derived from fractionation and variable degrees of crustal contamination. Triangles = footwall rocks, squares = hanging-wall rocks. B. The Genex synvolcanic mafic intrusion (diamonds) is derived from a mantle source with minimal crustal contamination and fractionation. The Genex synvolcanic intermediate intrusion (asterisks) is derived from a crustal-contaminated source.

different magma source than the mafic volcanic rocks in the Genex area or from the same source with less fractionation and crustal contamination. Identical fractionating phases and similar REE trends support the latter hypothesis. Thus, the synvolcanic mafic sill may not have an extrusive equivalent in the Genex stratigraphy.

Samples from the synvolcanic intermediate sill plot very near the average upper crust, suggesting that these samples are derived from a mafic parental magma that had experienced a significant degree of crustal contamination (Fig. 9B). These trends are similar to those from the Genex mafic volcanic rocks (Fig. 9A) and suggest derivation from a similar source.

Additional evidence for contamination is seen in the presence of older zircon xenocrysts in many of the volcanic units in the Abitibi region, suggesting that magmas commonly experienced contamination from older lithologic units (Ayer et al., 2005).

The Genex Mineralization

The Genex deposit is a Cu-Zn massive sulfide deposit that consists of three lenses of mineralization (the C, H, and A zones; Figs. 2, 3) that were mined from 1964 to 1966. All of the mill feed came from the C zone. Pyrite-chalcopyrite-sphalerite mineralization is also contained within numerous east-trending shears in both mafic and felsic rock types.

The C-zone pyrite-chalcopyrite mineralization is hosted in a north-trending mafic pillow breccia (Fig. 6E). Stringer mineralization is also present in pillow selvages and amygdules within flows in the stratigraphic footwall to the deposit. The stratigraphic hanging wall to the C zone is the upper synvolcanic mafic sill, and mineralization does not occur above this intrusion.

The H zone is a lens of dominantly pyrite-chalcopyrite mineralization that trends approximately east, perpendicular to stratigraphy. Mineralization occurs within the matrix of a felsic tuff and also at the contact of the tuff with the surrounding synvolcanic intermediate sill (Middleton, 1975). Locally, the mineralization occurs within the sill as disseminated stringers and massive zones, but without exception, it occurs no more than 30 m from the contact (Middleton, 1975).

The A zone is a small, east-trending lens of massive to stringer pyrite, chalcopyrite, and sphalerite located directly adjacent to the H zone but hosted dominantly in the intermediate sill (Fig. 6F). Some mineralization occurs in the felsic lapilli tuff (Middleton, 1975; Legault, 1985).

The Genex mineralization is interpreted to have been emplaced in the subsea floor within zones of higher primary permeability through processes of void-space filling and replacement. Evidence for this interpretation includes: (1) the occurrence of a stringer zone localized along pillow selvages and stratigraphically below the C-zone mineralization, (2) the occurrence of sulfides in areas of higher primary permeability, such as in pillow selvages and in the matrices of pillow breccias and lapilli tuffs, and (3) the stratiform nature of the major zone of mineralization (the C zone) without the presence of exhalite. The disconformable nature of the H and A zones suggests that the sulfides were deposited along fault zones. In the Genex area, faults likely represent conduits for not only the intermediate sill but also for the hydrothermal fluids.

The presence of mineralization in the lower fine-grained synvolcanic mafic sill, as well as in the synvolcanic intermediate sill, suggests that the two intrusions were emplaced before or during the mineralizing event. However, the upper fine-grained mafic sills are devoid of mineralization, which suggests that they may have been emplaced postmineralization.

The Genex Subvolcanic Intrusion

The large medium-grained mafic intrusion on the west side of the Genex area, near Forbes Lake (the Genex subvolcanic

intrusion; Fig. 3) and other identical intrusions to the northeast and southwest (Fig. 1) were grouped as one intrusive phase by Middleton (1975) who, along with Barrie and Davis (1990), Barrie et al. (1991, 1993), and Barrie (1992), included it as an upper phase of the Kamiskotia Gabbroic Complex. The upper phases of the Kamiskotia Gabbroic Complex have an age of 2704.8 ± 1.4 Ma, whereas the Genex stratigraphy has an age of 2698.6 ± 1.3 Ma (Hathway et al., 2005). The Genex subvolcanic intrusion cuts the 2698 Ma Genex stratigraphy and the older 2704 Ma Kamiskotia Gabbroic Complex succession, indicating that it is clearly younger and not part of the older Kamiskotia Gabbroic Complex. The Genex subvolcanic intrusion surrounding Forbes Lake and the other similar bodies to the northeast and southwest are identical mineralogically and geochemically to the fine-grained mafic synvolcanic sills within the Genex area. Thus, they are interpreted to be subvolcanic intrusions related to the 2698 Ma volcanic succession in the Genex area.

The size and postmineralization nature of the Genex subvolcanic intrusion suggests that it is neither large enough nor of an appropriate age to have provided the heat necessary to drive the hydrothermal system responsible for the Genex deposit and associated alteration (cf. Cathles et al., 1997).

Volcanic Reconstruction of the Genex Area

The Genex deposit is interpreted to have formed within a synvolcanic graben, the south margin of which lies east of the south end of Forbes Lake. Here, east-trending synvolcanic faults drop down felsic volcaniclastic rocks of unit 1, but do not offset the footwall synvolcanic mafic and intermediate sills, constraining subsidence to pre-sill emplacement. The north margin of the graben has not been spatially constrained.

Massive mafic sills and dikes within unit 2 are feeders to the overlying mafic flows and collectively they define a proximal mafic volcanic vent within the graben. The distribution and orientation of these earliest mafic intrusions is controlled by the east-west synvolcanic faults. The Genex mineralization is located within the mafic volcanic vent where it occurs as a strata-bound subsea-floor replacement of mafic volcaniclastic rocks (C zone) and as discordant veins and stringers within the mafic feeder dikes and along their contacts with the mafic volcanic flows (H and A zones).

The Genex deposit formed during the onset of mafic volcanism that followed the emplacement of a voluminous felsic volcaniclastic succession that, in turn, was followed by subsidence and the formation of the Genex graben. Mafic volcanism was followed by a period of relative volcanic quiescence marked by the emplacement of a thick succession of heterolithic volcaniclastic rocks and intercalated mudstone and siltstone, the deposition of which was interrupted by the eruption of thin basalt flows and localized rhyolite flows and/or domes. Assuming a relatively horizontal upper surface for the unit 2 mafic volcanic rocks, the thickening of this unit to the north suggests a broader area of subsidence, which includes the proposed Genex graben.

The footwall mafic and intermediate sills were emplaced during mafic volcanism, and the occurrence of stringer mineralization within these intrusions indicates that they were emplaced pre- or synmineralization. The hanging-wall mafic sills may have been emplaced during the waning stages of the eruption of unit 2 mafic flows or during volcanism that accompanied emplacement of unit 3. The larger, medium-grained, Genex subvolcanic intrusion located deeper in the footwall (to the west), and other similar intrusions to the northeast and southwest, truncate the footwall mafic intrusion and are interpreted to represent a resurgent stage of magmatism that postdated unit 3 and the Genex VMS mineralization.

Role of the Kamiskotia Gabbroic Complex

Campbell et al. (1981, 1982), Barrie and Davis (1990), Barrie et al. (1991, 1993), and Barrie (1992) have interpreted the Kamiskotia Gabbroic Complex as the subvolcanic pluton and the heat source that drove the hydrothermal convection cell responsible for the formation of four VMS deposits in the Kamiskotia area (Kam-Kotia, Canadian Jamieson, Genex, and Jameland; Fig. 1). Certainly the size, gabbroic composition (i.e., higher temperature), and interpreted level of emplacement for the Kamiskotia Gabbroic Complex favor it as a potential heat source. However, recent U-Pb geochronological work in the Kamiskotia Volcanic Complex (Fig. 1; Ayer et al., 2005; Hathway et al., 2008) indicates that the upper phases of the Kamiskotia gabbro (2704.8 ± 1.4 Ma) are older than a felsic crystal tuff from the base of the Genex stratigraphy (2698.6 ± 1.3 Ma). A slightly older age of 2703 ± 1.2 Ma (Tisdale age) was determined from a felsic volcanic rock in Turnbull Township within the Lower Kamiskotia Volcanic Complex, stratigraphically below the Genex stratigraphy (in Godfrey Township). An age of 2705 ± 2 Ma (Barrie and Davis, 1990), also Tisdale age and correlative with the Lower Kamiskotia Volcanic Complex, with error taken into account, was determined for a rhyolite in southwestern Godfrey Township. These ages indicate that the Kamiskotia Gabbroic Complex is at least 3.5 m.y. older than Upper Kamiskotia Volcanic Complex stratigraphy hosting the Genex deposit, thus precluding it from being the subvolcanic pluton to the Kamiskotia-Genex volcanic complex stratigraphy and the heat source that drove the hydrothermal system for the younger Genex, Kam-Kotia, Canadian Jamieson, and Jameland VMS deposits. Thus, the Kamiskotia Gabbroic Complex is now interpreted to represent a subvolcanic pluton related to the Lower Kamiskotia Volcanic Complex.

This approximately 3.5-m.y. time difference between the Kamiskotia Gabbroic Complex, including its host Lower Kamiskotia strata and Upper Kamiskotia strata that hosts the Genex deposit, may be represented by an unmapped disconformity or unconformity, a fault, or else the 3.5 m.y. is represented by <500 m of strata (Fig. 1). Mapping in the Genex area around Forbes Lake (Hocker et al., 2005) and between the Kamiskotia Gabbroic Complex and the Kam-Kotia deposit (Hathaway et al., 2008) has not identified a major unconformity or fault separating the Upper and Lower Kamiskotia Volcanic Complexes. However, the Genex subvolcanic intrusion that transects both the Lower and Upper Kamiskotia volcanic successions is not offset by a fault (Fig. 3), which suggests that the boundary between these two successions is either an unconformity or is conformable.

The thickness of the Lower Kamiskotia strata along the east margin of the Kamiskotia Gabbroic Complex is variable as shown in Figure 1. In the footwall to the Genex deposit, the

Lower Kamiskotia strata is approximately 3 km in thickness, whereas in the footwall to the Kam-Kotia, Canadian Jamieson, and Jameland VMS deposits, the Lower Kamiskotia strata ranges from <100 to <700 m in thickness. The level in the crust to which an intrusion rises is controlled by the magma driving force, lithostatic load (and hydrostatic load in submarine environments), and thermal gradient, with the thickness of an intrusion directly related to the thickness of the overlying strata (if the thickness of the intrusion were to exceed that of the cover rocks, lithostatic failure would occur and the magma would be erupted at surface: Johnson and Pollard, 1973; Corry, 1988; Roman-Berdiel et al., 1995; Hogan et al., 1998). Thus, as the Kamiskotia Gabbroic Complex is at least 2 to 3 km thick, it could not have been emplaced into such a thin (<700 m) succession of Lower Kamiskotia strata. This suggests that a significant thickness of the Lower Kamiskotia strata (perhaps several kilometers) north of the Steep Lake fault (Hathway et al., 2008, Fig. 1) was removed after emplacement of the Kamiskotia Gabbroic Complex and prior to eruption of the younger, Upper Kamiskotia strata. There is no evidence in the Lower or Upper parts of the Kamiskotia Volcanic Complex to indicate shallow water or above storm-wave base depositional environments, so removal of Lower Kamiskotia strata cannot be explained by subaerial erosion. One possible scenario to explain the missing Lower Kamiskotia strata is that this part of the Lower Kamiskotia Volcanic Complex underwent sector collapse and strata was removed and transported downslope, analogous to voluminous slides observed in modern volcanic arcs (e.g., Tonga arc: Worthington et al., 2003; Fig. 2). The emplacement of the Kamiskotia Gabbroic Complex into its own Lower Kamiskotia volcanic edifice during resurgent volcanism, as illustrated in Figure 10, may have, in part, triggered such a slide. In this scenario, the younger Upper Kamiskotia volcanic edifice would have been constructed on the collapsed remnants of the older Lower Kamiskotia edifice, with the two separated by a 3.5-m.y. depositional gap represented by an unconformity.

In the generally accepted hydrothermal model for formation of VMS deposits, hydrothermal circulation systems are driven by a high thermal gradient, which in some cases may be in response to, or manifest by, the emplacement of a high-level (2–4 km below sea floor) subvolcanic intrusion (Franklin, 1993, 1996; Galley, 1993, 1996). Based on thermal models by Cathles (1981), Cathles et al. (1997), and Barrie et al. (1999), the duration of a hydrothermal system is primarily a function of the mass of the intrusion, temperature of the magma, and depth of emplacement. In order to produce a moderate-sized VMS deposit of ~ 20 Mt, a magma chamber of 300 km^3 is required (cf. Cann et al., 1985). Thus the Genex subvolcanic intrusion is too small to drive the hydrothermal system responsible for the Genex deposit.

Although the Kamiskotia Gabbroic Complex is too old and the Genex subvolcanic intrusion is too small and may postdate mineralization, a heat source must have been present to account for four VMS deposits and several base metal occurrences in the Upper Kamiskotia strata located immediately above the Kamiskotia Gabbroic Complex. Galley (2003) and Hart et al. (2004) have suggested that although high-level subvolcanic plutons may postdate associated VMS deposits,

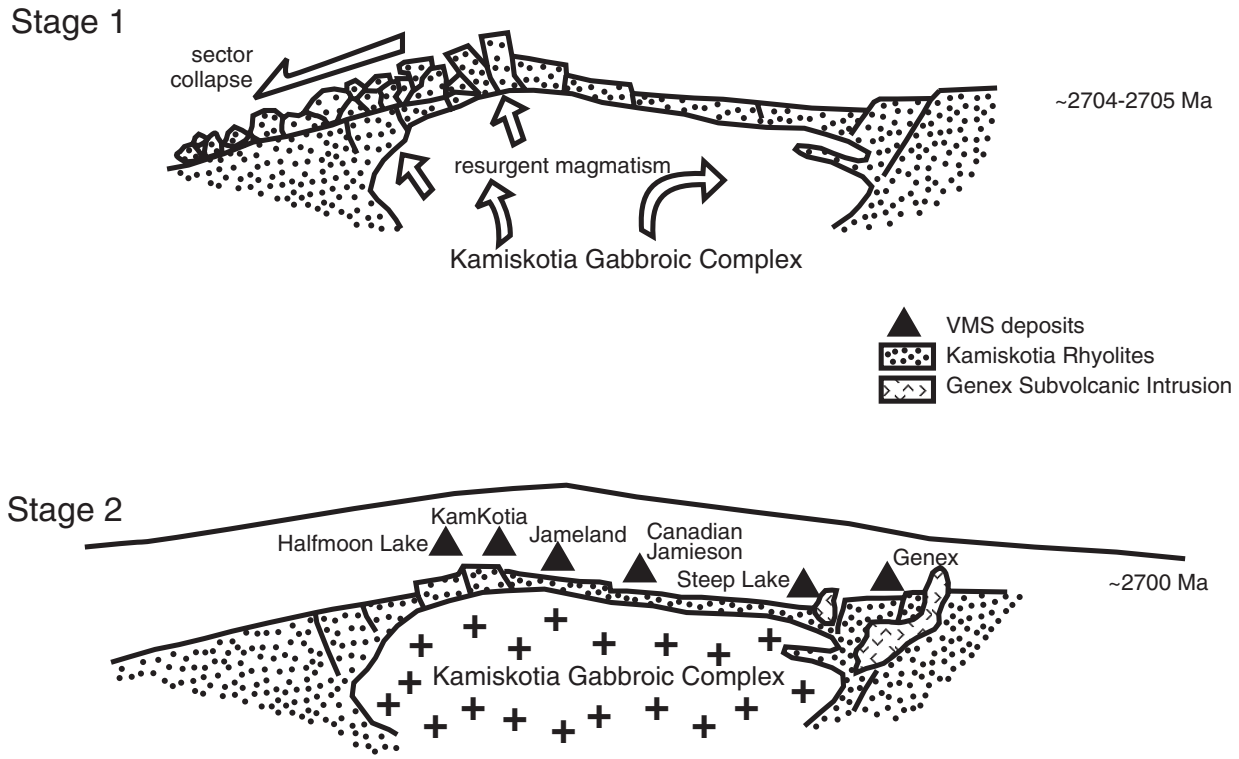

FIG. 10. Idealized sketch of the Kamiskotia Gabbroic Complex intruding Lower Kamiskotia strata (stage 1) causing gravitational collapse of a sector of the edifice (stage 2): Development of the Upper Kamiskotia strata, the Genex synvolcanic intrusion and related VMS mineralization.

they are commonly emplaced within long-lived high-temperature thermal corridors. In this case, the spatial coincidence of the Kamiskotia Gabbroic Complex, the 3.5-m.y. younger Genex subvolcanic intrusion, and superimposed Lower and Upper Kamiskotia volcanic centers indicates a long-lived thermal corridor that may have been ultimately responsible for establishing the high-temperature hydrothermal systems and VMS deposits.

Summary and Conclusions

Mafic and intermediate intrusions in the Genex area are synvolcanic and were emplaced syn- to postmineralization. The presence of peperite, a pillowed base, irregular contacts, amoeboid dikes, and incorporation of felsic volcaniclastic rocks all indicate that the mafic intrusions are high-level synvolcanic sills. The presence of a mixed zone, abundant spherulites and amygdules, and the utilization of the faults as conduits indicate that the intermediate intrusion is also a high-level synvolcanic intrusion but is slightly younger than the mafic intrusions.

The synvolcanic intrusions are not directly related to the Genex VMS mineralization but do indicate the presence of synvolcanic structures and a high heat-flow thermal regime. The high-level mafic intrusions previously grouped with the upper zones of the Kamiskotia Gabbroic Complex are interpreted to be younger and correlative with the Genex mafic synvolcanic intrusions. These synvolcanic intrusions collectively define a large subvolcanic dike and sill complex that was emplaced within Blake River-equivalent, Upper Kamiskotia strata of the Kamiskotia Volcanic Complex.

Based on new geochronological data, the large Kamiskotia Gabbroic Complex is older than the VMS-hosting Upper Kamiskotia strata and was emplaced into older, Lower Kamiskotia strata. The contact between the Lower and Upper Kamiskotia strata is interpreted to be an unconformity that spans approximately 3.5 m.y.

The older Kamiskotia Gabbroic Complex and the younger Genex synvolcanic intrusions do not share a common petrogenesis nor were they the heat source for the Genex hydrothermal alteration system. However, their spatial coincidence suggests that this part of the Kamiskotia Volcanic Complex was a focus of long-lived intrusive activity and high heat flow that defines a thermal corridor along which the known VMS deposits in the Kamiskotia Volcanic Complex were developed.

REFERENCES

Ayer, J., Amelin, Y., Corfu, F., Kamo, S., Ketchum, J., Kwok, K., and Trowell, N., 2002, Evolution of the southern Abitibi greenstone belt based on U-Pb geochronology: autochthonous volcanic construction followed by plutonism, regional deformation and sedimentation: Precambrian Research, v. 115, p. 63–95.

Ayer, J.A., Thurston, P.C., Bateman, R., Dube, B., Gibson, H.L., Hamilton, M.A., Hathway, B., Hocker, S., Houle, M., Hudak, G., Lafrance, B., Lesher, C.M., Ispolatov, V., MacDonald, P.J., Peloquin, A.S., Piercey, S.J., Reed, L.E., and Thompson, P.H., 2005, Overview of results from the Greenstone Architecture Project: Discover Abitibi Initiative: Ontario Geological Survey Open File Report 6154, 146 p.

Barrie, C.T., 1992, Geology of the Kamiskotia area: Ontario Geological Survey Open File Report 5829, 179 p.

Barrie, C.T., and Davis, D.W., 1990, Timing of magmatism and deformation in the Kamiskotia-Kidd Creek area, western Abitibi subprovince, Canada: Precambrian Research, v. 46, p. 217–240.

Barrie, C.T., Gorton, M.P., Naldrett, A.J., and Hart, T.R., 1991, Geochemical constraints on the petrogenesis of the Kamiskotia gabbroic complex and related basalts, western Abitibi subprovince, Ontario, Canada: Precambrian Research, v. 50, p. 173–199.

Barrie, C.T., Ludden, J.N., and Green, T.H., 1993, Geochemistry of volcanic rocks associated with Cu-Zn and Ni-Cu deposits in the Abitibi subprovince: Economic Geology, v. 88, p. 1341–1358.

Barrie, C.T., Cathles, L.M. and Erendi, A., 1999, Finite element heat and fluid-flow computer simulations of a deep ultramafic sill model for the giant Kidd Creek volcanic-associated massive sulfide deposit, Abitibi subprovince, Canada: Economic Geology Monograph 10, p. 529–540.

Binney, P., and Barrie, C.T., 1991, Kamiskotia area: Geological Survey of Canada Open File Report 2161, p. 52–65.

Campbell, I.H., Franklin, J.M., Gorton, M.P., Hart, T.R., and Scott, S.D., 1981, The role of subvolcanic sills in the generation of massive sulfide deposits: Economic Geology, v. 76, p. 2248–2253.

Campbell, I.H., Coad, P., Franklin, J.M., Gorton, M.P., Scott, S.D., Sowa, J., and Thurston, P.C., 1982, Rare earth elements in volcanic rocks associated with Cu-Zn massive sulphide mineralization: A preliminary report: Canadian Journal of Earth Sciences, v. 19, p. 619–623.

Cann, J.R., Strens, M.R., and Rice, A., 1985, A simple magma-driven thermal balance model for the formation of volcanogenic massive sulphides: Earth and Planetary Science Letters, v. 76, p. 123–134.

Cas, R.A.F., and Wright, J.V., 1988, Volcanic successions: Modern and ancient: London, Unwin Hyman, 529 p.

Cathles, L.M., 1981, Fluid flow and genesis of hydrothermal ore deposits: Economic Geology 75th Anniversary Volume, p. 424–457.

Cathles, L.M., Erendi, A.H.J., and Barrie, T., 1997, How long can a hydrothermal system be sustained by a single intrusive event?: Economic Geology, v. 92, p. 766–771.

Chown, E.H., Harrap, R., and Moukhsil, A., 2002, The role of granitic intrusions in the evolution of the Abitibi belt, Canada: Precambrian Research, v. 115, p. 291–310.

Corry, C.E., 1988, Laccoliths: Mechanics of emplacement and growth: Geological Society of America Special Paper 220, 110 p.

Dimroth, E., Cousineau, P., Leduc, M., and Sanschagrin, Y., 1978, Structure and organization of Archean subaqueous basalt flows, Rouyn-Noranda area, Quebec, Canada: Canadian Journal of Earth Sciences, v. 15, p. 902–918.

Dostal, J., and Mueller, W.U., 1997, Komatiite flooding of a rifted Archean rhyolitic arc complex: Geochemical signature and tectonic significance of the Stoughton-Roquemaure Group, Abitibi greenstone belt, Canada: Journal of Geology, v. 105, p. 545–463.

Doyle, M.G., and Allen, R.L., 2003, Subsea-floor replacement in volcanic-hosted massive sulfide deposits: Ore Geology Reviews, v. 23, p. 183–222.

Ernst, R.E., 1981, Correlation of Precambrian diabase dike swarms across the Kapuskasing structural zone, northern Ontario: Unpublished M.Sc. thesis, Ontario, University of Toronto, 184 p.

Fisher, R.V., 1966, Rocks composed of volcanic fragments and their classification: Earth-Science Reviews, v. 1, p. 287–298.

Franklin, J.M., 1993, Volcanic-associated massive sulphide deposits: Geological Association of Canada Special Paper 40, p. 315–334.

———1996, Volcanic-associated massive sulphide base metals: Geology of Canada, Geological Survey of Canada, no. 8, p. 158–183.

Galley, A.G., 1993, Characteristics of semi-conformable alteration zones associated with volcanogenic massive sulfide districts: Journal of Geochemical Exploration, v. 48, p. 175–200.

———1996, Geochemical characteristics of subvolcanic intrusions associated with Precambrian massive sulphide districts: Geological Association of Canada Short Course Notes, v. 12, p. 239–278.

———2003, Composite synvolcanic intrusions associated with Precambrian VMS-related hydrothermal systems: Mineralium Deposita, v. 38, p. 443–473.

Gibson, H.L., Morton, R.L., and Hudak, G.J., 1999, Submarine volcanic processes, deposits, and environments favorable for the location of volcanic-associated massive sulfide deposits: Reviews in Economic Geology, v. 8, p. 13–51.

Gibson, H.L., Ames, D., Bailes, A., Tardif, N., Devine, C., Galley, A., and Maclachlan, K., 2003, Invasive flows, peperite and Paleoproterozoic massive sulfide, Flin Flon, Manitoba and Saskatchewan [abs.]: Geological Association of Canada-Mineralogical Association of Canada Joint Annual Meeting, Vancouver, Canada, Abstracts, v. 28, unpaginated.

Hart, T., Gibson, H. J., and Lesher, C. M., 2004, Trace element geochemistry and petrogenesis of felsic volcanic rocks associated with volcanogenic Cu-Zn-Pb massive sulfide deposits: Economic Geology, v. 99, p. 1003–1113.

Hathway, B., Hudak, G., and Hamilton, M.A., 2005, Geological setting of volcanogenic massive sulphide mineralization in the Kamiskotia area: Discover Abitibi Initiative: Ontario Geological Survey Open File Report 6155, 81 p.

Hathway, B., Hudak, G., and Hamilton, M.A., 2008, Geologic setting of volcanic-associated massive sulfide deposits in the Kamiskotia area, Abitibi subprovince, Canada: Economic Geology, v. 103, p. 1185–1202.

Heaman, L.M., 1988, A precise U-Pb zircon age for a Hearst dike [abs.]: Geological Association of Canada-Mineralogical Association of Canada, Program with Abstracts, v. 13, p. A53.

Hocker, S.M., 2005, Volcanic stratigraphy, synvolcanic intrusions and control on mineralization at the Archean Genex mine, Kamiskotia area, Timmins, Ontario: Unpublished M.Sc. thesis, Sudbury, Ontario, Laurentian University, 215 p.

Hocker, S.M., Thurston, P.C., and Gibson, H.L., 2005, Volcanic stratigraphy and controls on mineralization in the Genex mine area, Kamiskotia area: Discover Abitibi Initiative: Ontario Geological Survey Open File Report 6156, 143 p.

Hogan, J.P., Price, J.D., and Gilbert, M.C., 1998, Magma traps and driving pressure: Consequences for plutonic shape and emplacement in an extensional regime: Journal of Structural Geology, v. 20, p. 1155–1168.

Houlé, M.G., Gibson, H.L., Lesher, C.M., Davis, P.C., Cas, R.A.F., Beresford, S.W., and Arndt, N.T., 2008, Komatiitic sills and multigenerational peperite at Dundonald Beach, Abitibi greenstone belt, Ontario: Volcanic architecture and nickel sulfide distribution: Economic Geology, v. 103, p. 1269–1284.

Johnson, A.M., and Pollard, D.D., 1973, Mechanics of growth of some laccolithic intrusions in the Henry Mountains, Utah, Part I: Tectonophysics, v. 18, p. 261–309.

Legault, M.H., 1985, The geology and alteration associated with the Genex volcanogenic Cu massive sulphide deposit, Godfrey Township, Timmins, Ontario: Unpublished M.Sc. thesis, Ottawa, Ontario, Carleton University, 222 p.

Lydon, J.W., 1988, Ore deposit models #14: Volcanogenic massive sulphide deposits, Part 2: Genetic models: Geoscience Canada, v. 15, p. 43–65.

MacDonald, P.J., Piercey, S.J., and Hamilton, M.A., 2005, An integrated study of intrusive rocks spatially associated with gold and base metal mineralization in Abitibi greenstone belt, Timmins area and Clifford Township: Discover Abitibi Initiative: Ontario Geological Survey Open File Report 6160, 210 p.

Middleton, R.S., 1975, Geology of Turnbull and Godfrey Townships, District of Cochrane: Ontario Division of Mines Open File Report 5118, 267 p.

Mueller, W.U., and Mortensen, J.K., 2002, Age constraints and characteristics of subaqueous volcanic construction, the Archean Hunter Mine Group, Abitibi greenstone belt: Precambrian Research, v. 115, p. 119–152.

Osmani, I.A., 1991, Proterozoic mafic dike swarms in the Superior province of Ontario: Ontario Geological Survey Special Volume 4, Part 1, p. 661–681.

Pearce, J.A., 1996, A user's guide to basalt discrimination diagrams: Geological Association of Canada Short Course Notes, v. 12, p. 79–113.

Pearce, J.A., and Cann, J.R., 1973, Tectonic setting of basic volcanic rocks determined using trace element analysis: Earth and Planetary Science Letters, v. 19, p. 290–300.

Rollinson, H.R., 1993, Using geochemical data: Evaluation, presentation, interpretation: Harlow, England, Prentice Hall, 352 p.

Roman-Berdiel, T., Gapais, D., and Brun, J.P., 1995, Analogue models of laccolith formation: Journal of Structural Geology, v. 17, p. 1337–1346.

Setterfield, T.N., Hodder, R.W., Gibson, H.L., and Watkins, J.J., 1995, The McDougall-Despina fault set, Noranda, Quebec: Evidence for fault-controlled volcanism and hydrothermal fluid flow: Exploration and Mining Geology, v. 4, p. 381–393.

Stix, J., Kennedy, B., Hannington, M., Gibson, H., Fiske, R., Mueller, W., and Franklin, J., 2003, Caldera-forming processes and the origin of submarine volcanogenic massive sulfide deposits: Geology, v. 31, p. 375–378.

Sun, S-S., and McDonough, W.F., 1989, Chemical and isotopic systematics of oceanic basalts: Implications for mantle composition and processes: Geological Society of London Special Publication 42, p. 313–345.

Troll, V.R., Emeleus, C.H., and Donaldson, C.H., 2000, Caldera formation in the Rum Central Igneous Complex, Scotland: Bulletin of Volcanology, v. 62, p. 301–317.

White, J.D.L., 2000, Subaqueous eruption-fed density currents and their deposits: Precambrian Research, v. 101, p. 87–109.

Worthington, T., Stoffers, P., Hekinian, R., Ackermand, D., Bigalke, N., Timm, C., Tonga'onevai, S., Unverrict, D., Vailea, A., and Zimmer, M., 2003, Structure and petrology of the South Tonga arc: Cruise Report SONNE 167, Louisville, Berichte-Reports Institut für Geowissenchaften 20, p. 11–89.

Wyman, D.A., Kerrich, R., and Polat, A., 2002, Assembly of Archean cratonic mantle lithosphere and crust: Plume-arc interaction in the Abitibi-Wawa subduction-accretion complex; Precambrian Research, v. 115, p. 37–62.